Allergy and Immunology

http://www.aimspress.com/journal/Allergy/

AIMS Allergy and Immunology, 7(4): 281–303
DOI: 10.3934/Allergy.2023019
Received: 17 August 2023
Revised: 01 December 2023
Accepted: 04 December 2023
Published: 20 December 2023

Research article

Enhancing the efficacy of anti-malarial drugs with immune boosters: A mathematical model

Dorcas Mulenga[1], Winnie Anoumedem[2], Blessing O. Emerinini[3] and Nourridine Siewe[1,3,*]

[1] African Institute for Mathematical Sciences (AIMS)-Cameroon, Limbe, SWR, Cameroon
[2] Hôpital de Djoungolo, Yaoundé, CR, Cameroon
[3] School of Mathematics and Statistics, College of Science, Rochester Institute of Technology, Rochester, NY, USA

* **Correspondence:** Email: nourridine@aims.ac.za; Tel: +15854757605; Fax: +15854757605.

Abstract: This paper presents a mathematical model of severe malarial anemia (SMA), which is a complication of malaria and is a major contributor to malaria-related deaths. SMA is characterized by a decrease in hemoglobin levels in the blood due to the suppression of red blood cell (RBC) recruitment by the protein macrophage migration inhibitory factor (MIF). Plasmodium falciparum, which is a malaria-causing parasite, secretes a specific form of MIF called plasmodium falciparum macrophage migration inhibitory factor (PFMIF), which affects immune cells. Artesunate, which is the primary treatment for SMA, reduces the parasite level but does not increase hemoglobin levels and can sometimes lead to hemolytic anemia, which requires a blood transfusion. To address this issue, the experimental drug Epoxyazadiradione (Epoxy) was explored as a potential treatment for SMA. Epoxy inhibits both MIF and PFMIF interactions with immune cells and has the potential to increase hemoglobin levels in SMA patients. Our model simulations support previous findings that the appropriate combination of Artesunate with Epoxy can reduce parasite load while preventing anemia by maintaining hemoglobin levels at an adequate level. Additionally, we explored the impact of immune boosters on the anti-malarial drugs Artesunate and Epoxy and discovered that an insufficient amount of drugs is ineffective, while an excessive amount may not be beneficial.

Keywords: severe malarial anemia; Artesunate; Epoxyazadiradione; hemoglobin level; parasitemia; MIF/PFMIF; immune booster

1. Introduction

Malaria is an infectious, vector-borne disease caused by a parasite native to the African continent, and it claims the lives of many humans each year, particularly children under the age of 5 [1, 2].

According to the World Health Organization's 2021 report, an estimated 241 million cases of malaria and 627,000 deaths were recorded that year. A significant challenge lies in controlling malaria to lower mortality and morbidity rates. The female Anopheles mosquito serves as a vector for malaria transmission, and the parasite responsible for the disease belongs to the *Plasmodium* family [3, 4]. The four types of *Plasmodium* that affect humans are *Plasmodium* vivax, *Plasmodium* falciparum, *Plasmodium* malariae, and *Plasmodium* ovale. The primary causative agent of malaria is *Plasmodium* falciparum. Malaria is transmitted when a female Anopheles mosquito injects the parasite into the bloodstream of an uninfected human. Conversely, the mosquito becomes infected after ingesting a blood meal from an infected human [5]. The mosquito species that are responsible for malaria prefer biting pregnant women, people with a higher body mass index, and individuals with the blood type O [6].

After being bitten by an infected Anopheles mosquito, the parasites, in the form of sporozoites, travel through the bloodstream to the liver cells, specifically hepatocytes, where they mature into schizonts. This stage is referred to as the mosquito liver stage [7]. The schizonts replicate within the liver cells in the form of merozoites, which are released into the bloodstream by ruptured hepatocyte cells. In the blood, the merozoites invade the red blood cells (RBCs) and multiply again within the RBCs to form more merozoites. After 1 to 2 weeks, the schizont ruptures, thereby releasing the merozoites into the bloodstream [8]. If left untreated at this stage, the cycle will persist, and the infected person will start developing symptoms of malaria, such as chills, fever, and sweating [9]. This stage is known as the mosquito blood stage. In addition to that, the merozoites develop into sexual forms known as gametocytes, which are taken up by the mosquitoes during blood meal in order to maintain the parasite life cycle [9, 10]. In this work, we will not consider the mosquito stage, which is the parasite's life cycle inside a mosquito. There are three stages of the parasite life cycle: the liver stage, the blood stage and the mosquito stage.

The rapid increase in parasites activates the immune system's mechanism. In response, the immune cells secrete an innate cytokine called the macrophage migration inhibitory factor (MIF), which regulates the immune responses and cell differentiation, a process in which immature cells acquire unique characteristics and mature into specialized forms with distinct functions. However, in severe malaria anemia, MIF contributes to the destruction of healthy red blood cells and a decrease in hemoglobin levels [11, 12]. In return, the parasites secrete a protein called *Plasmodium* Falciparum MIF (PFMIF), which hinders the invading activity and antigen presentation capabilities of the immune cells such as macrophages and dendritic cells [13,14]. This means that the body's immune system will not be able to distinguish between the body's cells and foreign cells, thereby promoting the survival and replication of the malaria parasite within the blood. Artesunate is a successful treatment for severe malaria anemia because it can block the growth and reproduction of the malaria parasites, which, in turn, prevents the destruction of the RBCs [15].

Despite Artesunate's efficacy in decreasing parasite load, there have been some reports concerning its use. Occasionally, Artesunate use might lead to hemolytic anemia, a condition where the destruction of RBCs is faster than the production, which results in the reduction of hemoglobin levels [16]. However, we can use Artesunate in conjunction with another antimalarial drug called Epoxyazadiradione (Epoxy), which is a naturally occurring substance present in neem trees that is known to have antimalarial drug characteristics. Epoxy has the ability to prevent the formation of MIF in human

monocytes, which are involved in the immune response to infections. Additionally, Epoxy can regulate immune cells and cytokines, such as PFMIF, and may help boost RBCs count [17]. By combining Artesunate and Epoxy in this study, we aim to reduce parasites while increasing hemoglobin levels.

Immune boosters are substances, strategies, or interventions that either enhance or strengthen the body's immune system, helping it to better defend against infections and diseases. A robust immune system is essential for a person's overall health and well-being [18–20]. The use of immune boosters in the context of malaria treatment is a complex and evolving area of research. While some immune-boosting strategies have shown promise in enhancing the body's response to malaria [18], it is important to note that the field of immuno-modulation in malaria is continually evolving, and the effectiveness of specific immune boosters may vary based on factors such as the parasite species and host immunity [19, 20].

In this paper, we developed a mathematical model of the human blood-stage *Plasmodium* life cycle. The model, which is based on and simplifies a previous work [21], is represented by a system of ordinary differential equations (ODEs). In this updated model, we have excluded the IL-12, IFN-γ, and TNF-α cytokines from the model in [21], and have reformulated the model network and system of equations accordingly. Subsequently, we employed this model to evaluate the effectiveness of treatment with the drugs Artesunate and Epoxy, both as individual therapies and in combination. Additionally, we investigated the role of immune boosters in the context of malaria treatment using these two drugs.

The rest of this paper is organized as follows. In Section 2, we develop the mathematical model designing the model network, then we write and describe the equations associated with this network. In Section 3, we present the results and model simulations, and the conclusion and recommendations are presented in Section 4.

2. Mathematical model

The mathematical model is based on the network in Figure 1. This network is a simplification of Figure 1 in [21], where we dropped the dendritic cells (antigen-presenting cells) and combined the effect of the immune response (represented in [21] by macrophages and Th1-cells) by lumping them together into one variable T_c. Furthermore, we dropped the IL-12, IFN-γ, and TNF-α cytokines and modeled their regulating effects by a constant parameter. The model parameters and their descriptions can be found in Table 2. Table 1 lists our model's variables in units of g/ml.

Table 1. Descriptions of variables (Vars) used in the model. All variables are in units of g/ml.

Vars	Descriptions	Vars	Descriptions
T_c	Density of $CD4^+$ T cells	B	Density of healthy RBCs
B_i	Density of infected RBCs	H_b	Concentration of hemoglobin
P_i	Intracellular parasite load	P_e	Extracellular parasite load
P_f	Concentration of PFMIF	M_f	Concentration of MIF
A	Concentration of artesunate	E	Concentration of epoxyazadiradione

Table 2. List of model's parameter values.

Parameters	Descriptions	Values	References
λ_B	The rate of release of B by B_0	1.15×10^{-2} d^{-1}	est. & HT
λ_{BB_i}	The rate of infection of B	6×10^{1} ml/g d^{-1}	HT
λ_{P_i}	The rate of growth of P_i in B_i	0.8 d^{-1}	HT
$\lambda_{P_iP_e}$	The rate of rupturing of B_i	0.66 d^{-1}	[21] & HT
$\lambda_{B_iT_c}$	The rate of ingestion of B_i by T_c	1.5602×10^{-6} ml/g d^{-1}	est.
$\lambda_{P_iT_c}$	The rate of ingestion of P_i by T_c	4.845×10^{-8} d^{-1}	est.
$\lambda_{P_eT_c}$	The rate of ingestion of P_e by T_c	2.425×10^{-7} d^{-1}	est.
$\lambda_{T_cP_e}$	The rate of activation of T_c by P_e	1×10^{3} d^{-1}	est.
$\lambda_{T_cP_i}$	The rate of activation of T_c by P_i	5×10^{2} d^{-1}	est.
$\lambda_{T_cB_i}$	The rate of activation of T_c by B_i	5×10^{2} d^{-1}	est.
$\lambda_{M_fT_c}$	The rate of secretion of M_f by T_c	6.71×10^{-5} d^{-1}	[21] & HT
$\lambda_{P_fP_i}$	The rate of secretion of P_f by P_i	2×10^{-3} d^{-1}	[21] & HT
$\lambda_{B_0M_f}$	The rate of absorption of M_f by B_0	3.9×10^{1} d^{-1}	[21] & HT
λ_{AB_i}	The rate of florescence of A in B_i	2.08×10^{-6} d^{-1}	[21]
λ_{EB}	The rate of florescence of E in B	1.2×10^{-9} d^{-1}	[21] & HT
λ_{ET_c}	The rate of florescence of E in T_c	1.2×10^{-9} d^{-1}	[21] & HT
μ_B	The rate of death healthy RBCs	5.78×10^{-3} d^{-1}	est.
μ_{B_i}	The rate of death of infected RBCs	5.78×10^{-3} d^{-1}	HT
μ_{P_e}	The rate of death of extracellular parasites	4.9×10^{2} d^{-1}	HT
μ_{T_c}	The rate of death of CD4$^+$ T cells	5×10^{-5} d^{-1}	HT
$\mu_{T_cP_f}$	Death rate of T_c by PFMIF	2×10^{-3} d^{-1}	HT
μ_{M_f}	Decay rate of MIF	1.39 d^{-1}	[21] & HT
μ_{P_f}	Decay rate of PMIF	2 d^{-1}	HT
μ_{B_iA}	Death rate of infected RBCs by A	0.1 d^{-1}	HT
μ_A	Degradation rate of Artesunate	33 d^{-1}	[21] & HT
μ_E	Degradation rate of epoxyazadiradione	1.98 d^{-1}	[21] & HT
B_0	RBCs in healthy human	0.45 g/ml	[21]
T_c^0	T cells in healthy human	1.08×10^{-3} g/ml	[21]
H_b	Hemoglobin in healthy human	0.14 g/ml	[21]
m_B^*	(mass of *Plasmodium* parasite)/(mass of RBC)	3.7×10^{-3}	[21]
m_{M_f}	(mass of MIF)/(mass of *RBC*)	7.78×10^{-10}	HT
N_B	Average number of P_i released per burst of B_i	24	[21]
n_B	Average number of P_i in one iRBC	6	[21]
θ_H	Fraction of hemoglobin in iRBCs	0.33	[21]
K_{B_i}	Half-saturation of B_i	0.015 g/ml	[21]
K_{T_c}	Half-saturation of T_c	1.08×10^{-3} g/ml	[21]
K_{P_e}	Half-saturation of P_e	4×10^{-4} g/ml	[21]
K_{P_i}	Half-saturation of P_i	1.3×10^{-3} g/ml	[21]
K_{M_f}	Half-saturation of MIF	4×10^{-9} g/ml	[21]
K_{P_f}	Half-saturation of PFMIF	8×10^{-10} g/ml	[21]
K_A	Half-saturation of A	3.26×10^{-6} g/ml	[21]
K_E	Half-saturation of E	4×10^{-6} g/ml	[21]
C_a	Carrying capacity of P_i	2.6×10^{-3} g/ml	[21]

est. = estimated, HT = hand tuned (refer to Section A).

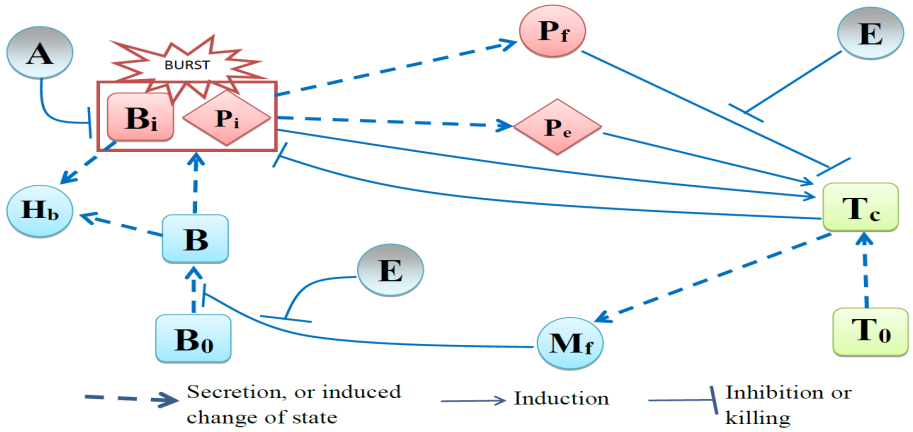

Figure 1. A network is used to represent the interaction between cells, parasites and anti-malarial drugs during treatment. See Table 1 for the description of each variable.

Following the model by Siewe and Friedman [21], the model is based on the following assumptions:

(i) During a malaria infection, various types of immune cells are activated in response to the presence of parasites in the body. In our model, we assume that the immune system consists of a single compartment, namely CD4$^+$ T cells (T_c).

(ii) Red blood cells (RBCs) are produced by spongy-like structures called bone marrow, which are found within bones, at a rate of λ_B. They are reduced by infection from extracellular merozoites at a rate of λ_{BB_i}.

(iii) The merozoite form of intracellular parasites replicates inside healthy red blood cells while circulating in the blood at a rate of λ_{P_i}.

(iv) When red blood cells are invaded by intracellular merozoites and replicate inside them, it results in the rupture of the infected red blood cells at a rate of $\lambda_{P_iP_e}$.

(v) The presence of the intracellular and extracellular merozoites, as well as infected RBCs in the bloodstream, triggers the body to produce immune cells called CD4$^+$ T cells at the rates of $\lambda_{T_cP_e}$, $\lambda_{T_cP_i}$ and $\lambda_{T_cB_i}$.

(vi) In turn, the CD4$^+$ T cells kill the infected RBCs together with the intracellular and extracellular parasites at the rates of $\lambda_{T_cB_i}$, $\lambda_{T_cP_i}$ and $\lambda_{T_cP_e}$, respectively.

(vii) T cells secrete MIF, which participates in inflammatory and immune responses at a rate of $\lambda_{M_fT_c}$. MIF suppresses red blood cells, thereby leading to the depletion of hemoglobin.

(viii) Lastly, intracellular parasites secrete PFMIF at a rate of $\lambda_{P_fT_c}$.

2.1. Equation for healthy red blood cells (B)

After the release of healthy red blood cells from the bone marrow, MIF interferes with the process, as shown by the first term on the right-hand side [22]. The ratio $1/(1 + E/K_E)$ is the inhibitory effect of MIF by the drug Epoxy. The second term describes the rate of infection of healthy RBCs, denoted

by λ_{BB_i}, thereby leading to a reduction in healthy red blood cells and an increase in infected red blood cells B_i [23]. The last term represents the natural death of the RBCs. Hence, the equation of B is given by the following:

$$\frac{dB}{dt} = \underbrace{\lambda_B B_0 \frac{1}{(1 + M_f/K_{M_f})\frac{1}{1 + E/K_E}}}_{\text{Release}} - \underbrace{\lambda_{BB_i} B P_e}_{\text{Infection}} - \underbrace{\mu_B B.}_{\text{death}} \tag{2.1}$$

2.2. Equation for infected red blood cells (B_i)

When extracellular parasites invade red blood cells, there is an increase in the number of infected RBCs [24]. We assume that bursting occurs when the concentration of intracellular parasites P_i is roughly the same as $m_B^* N_B B_i$, where N_B represents the number of parasites released per burst, and m_B^* represents the mass of one plasmodium parasite cell over the mass of one RBC. The reduction in infected RBCs is a result of the phagocytosis of T_c cells [25], as shown in the "ingestion" term below.

The last two terms represent the rate of death of infected RBCs by the drug Artesunate (when administered) [26] and by natural death, respectively. Hence, B_i satisfies the following equation:

$$\frac{dB_i}{dt} = \underbrace{\lambda_{BB_i} B P_e}_{\text{infection}} - \underbrace{\lambda_{P_i P_e} B_i \frac{P_i^2}{(m_B^* N_B B_i)^2 + P_i^2}}_{\text{Bursting}} - \underbrace{\lambda_{B_i T_c} T_c B_i}_{\text{ingestion}} - \underbrace{\mu_{B_i A} \frac{A}{K_A + A} B_i}_{\text{death by Artesunate}} \tag{2.2}$$

$$- \underbrace{\mu_{B_i} B_i}_{\text{natural death}},$$

where $m_B^* = \frac{\text{mass of 1 parasite}}{\text{mass of 1 RBC}}$.

2.3. Equation for intracellular parasites in the RBCs (P_i)

An increase in the intracellular parasite population is a result of their replication within B_i [27]. The replication rate is determined by the factor $1 - P_i/C_a$, which ensures that the concentration of intracellular parasites P_i does not exceed the carrying capacity C_a. Additionally, an increase in parasite numbers comes from new infections [28]. Additionally, the model accounts for a decrease in the number of parasites due to the rupture of infected RBCs ("bursting") [29]. The death rate of intracellular parasites [30] is enhancing T cells [31] and the action of the drug Artesunate when it is administered [21]. We represent the equation for P_i as follows:

$$\frac{dP_i}{dt} = \underbrace{\lambda_{p_i} P_i \left(1 - \frac{P_i}{C_a}\right)}_{\text{growth in } B_i} + \underbrace{\lambda_{BB_i} m_B^* B P_e}_{\text{infection}} - \underbrace{\lambda_{P_i P_e} m_B^* N_B B_i \frac{P_i^2}{(m_B^* N_B B_i)^2 + P_i^2}}_{\text{Bursting}} \tag{2.3}$$

$$- \underbrace{\lambda_{P_i T_c} \frac{P_i}{K_{P_i} + P_i} T_c}_{\text{Killed by } T_c} - \underbrace{\mu_{B_i A} n_B \frac{A}{K_A + A} B_i}_{\text{death by Artesunate}} - \underbrace{\mu_{B_i} n_B P_i}_{\text{death}}$$

where the constant n_B represents the number of intracellular parasites within one infected RBC at the time of its death due to natural cell death.

2.4. Equation for extracellular parasites (P_e)

We similarly represent the killing of P_e by T_c as in Eq (2.3), and extracellular parasites die naturally. It is worth noting that the constant n_B represents the number of intracellular parasites within one infected RBC at the time of its death due to natural cell death. We write the equation for P_e as follows:

$$\frac{dP_e}{dt} = \underbrace{\lambda_{P_iP_e} m_B^* N_B B_i \frac{P_i^2}{(m_B^* N_B B_i)^2 + P_i^2}}_{\text{Bursting}} - \underbrace{\lambda_{BB_i} m_B^* B P_e}_{\text{infection}} - \underbrace{\lambda_{P_eT_c} \frac{P_e}{K_{P_e} + P_e} T_c}_{\text{killed by } T_c} - \underbrace{\mu_{P_e} P_e}_{\text{death}}. \tag{2.4}$$

2.5. Equation for the CD4$^+$ T cells (T_c)

Activation of the naive CD4$^+$ T cells is triggered by infected RBCs B_i [32], intracellular P_i and extracellular P_e parasites, respectively. The T_c cells die naturally [33] and there is an augmented death rate of T_c resulting from the effect of PFMIF [12]; we represent this rate by $\mu_{T_cP_f} P_f/(K_{P_f} + P_f)$. When the drug Epoxy is administered, we represent its inhibition effect on PFMIF by the ratio $1/(1 + E/K_E)$. Hence,

$$\begin{aligned} \frac{dT_c}{dt} = & \underbrace{\left(\lambda_{T_cB_i} \frac{B_i}{K_{B_i} + B_i} + \lambda_{T_cP_i} \frac{P_i}{K_{P_i} + P_i} + \lambda_{T_cP_e} \frac{P_e}{K_{P_e} + P_e}\right) T_c^0}_{\text{proliferation}} \\ & - \underbrace{\left(\mu_{T_c} + \mu_{T_cP_f} \frac{P_f}{K_{P_f} + P_f} \frac{1}{1 + E/K_E}\right) T_c}_{\text{death}} \end{aligned} \tag{2.5}$$

where T_c^0 is the source of T_c cells.

2.6. Equation for MIF (M_f)

MIF is secreted by the CD4$^+$ T cells [34]. MIF is absorbed by inhibiting the production of red blood cells [35]. Hence, the equation for M_f is given as follows:

$$\frac{dM_f}{dt} = \underbrace{\lambda_{M_fT_c} T_c}_{\text{secretion}} - \underbrace{\lambda_{B_0M_f} m_{M_f}^* B_0 \frac{M_f}{K_{M_f} + M_f}}_{\text{absorption by } B_0} - \underbrace{\mu_{M_f} M_f}_{\text{decay}}. \tag{2.6}$$

where the third term on the right hand side is the natural decay of MIF.

2.7. Equation for PFMIF (P_f)

PFMIF is secreted by the intracellular parasites P_i [36] at rate $\lambda_{P_fP_i} P_i$. PFMIF decreases as it is absorbed by T_c. P_f also decays naturally [37]. Hence, the equation for P_f is written in the following form:

$$\frac{dP_f}{dt} = \underbrace{\lambda_{P_fP_i} P_i}_{\text{secretion}} - \underbrace{\mu_{T_cP_f} \frac{P_f}{K_{P_f} + P_f} T_c}_{\text{absorbed by T cells}} - \underbrace{\mu_{P_f} P_f}_{\text{decay}}. \tag{2.7}$$

2.8. Equation for hemoglobin (H_b)

Hemoglobin is a red pigment found in red blood cells that is responsible for the circulation of oxygen. We consider the total hemoglobin H_B equation to be as follows:

$$H_b = H_B(\mathrm{B} + B_i \times \theta_H), \tag{2.8}$$

as in [21], where H_B is the fraction of the hemoglobin level in healthy RBCs (B). We take the same percentage for infected RBCs, where B is the concentration of healthy RBCs, which is approximately 4.5 to 5.5×10^6 cells/ml or approximately 0.45 g/ml, and B_i is the concentration of infected RBCs, which can be as high as 20% to 50% of the total RBCs count or approximately 0.015 g/ml, from Table 2 [38]. Furthermore, θ_H is the constant rate of hemoglobin consumed by malaria parasites. The parasites consume a constant rate of Hb to sustain their growth and reproduction, which is approximately 70% of the hemoglobin present in infected red blood cells (iRBCs). In healthy individuals, the percentage of Hb in RBCs is usually around 33% of the total volume of RBCs. However, in severe cases of malaria anemia, the percentage of hemoglobin in infected RBCs can be significantly lower than that of healthy RBCs [39].

The following result from Siewe and Friedman [40] establishes the well-posedness of the model's equations.

Theorem 2.1. *Consider the following system of differential equations:*

$$\frac{dx_i}{dt} = f_i(x_1, \ldots, x_n), \quad 1 \le i \le n, \tag{2.9}$$

and assume that the f_i's are continuously differentiable functions satisfying the following conditions in the nonnegative quadrant:

$$x_1 \ge 0, \quad x_2 \ge 0, \quad \ldots, \quad x_n \ge 0;$$

(1) $f_i(x_1, \ldots, x_n) < A + B\sum_{j=1}^{n} x_j$

(2) $f_i(x_1, \ldots, x_n) = g_i(x_1, \ldots, x_n) + h_i(x_1, \ldots, x_n)x_i$, *where*

(3) $g_i(x_1, \ldots, x_n) \ge 0$ *and* $h_i(x_1, \ldots, x_n) \ge -A_1 - B_1\sum_{j=1}^{n} x_j$, *with some positive constants A, B,* A_1 *and* B_1. *If* $x_i(0) > 0$ *for* $1 \le i \le n$, *then*

(4) $0 < x_i(t) < \frac{A}{B} + \hat{X}e^{nBt}$, *for* $1 \le i \le n$ *and all* $t > 0$, *where* $\hat{X} = \sum_{j=1}^{n} x_i(0)$.

Proof. The inequality (4) certainly holds if t is small. Hence, if the assertion (4) is not true, then there is a smallest time τ such that (4) holds for $t < \tau$ but not for $t = \tau$. To derive a contradiction, we start by using (1), alongside the following:

$$\frac{dx_i}{dt} \le A + B\sum_{j=1}^{n} x_j. \tag{2.10}$$

Setting $z = \sum_{j=1}^{n} x_j$, we obtain the following:

$$\frac{dz}{dt} \le nA + nBz, \quad \text{for } t < \tau. \tag{2.11}$$

Hence,

$$z(\tau) \leq e^{nB\tau} z(0) + \frac{A}{B}(1 - e^{-nB\tau}) \tag{2.12}$$

$$< \frac{A}{B} + \hat{X} e^{nB\tau}; \tag{2.13}$$

therefore, the second inequality in (4) follows with t = τ. Next, we use the conditions (2) and (3) to obtain de following:

$$\frac{dx_i}{dt} \geq -\Big(A_1 + B_1 \sum_{j=1}^{n} x_j\Big) x_i. \tag{2.14}$$

By the second inequality in (4),

$$A_1 + B_1 \sum_{j=1}^{n} x_j(t) \leq A_1 + nB_1\Big(\frac{A}{B} + \hat{X} e^{nB\tau}\Big) \equiv C, \quad \text{for } t \leq \tau. \tag{2.15}$$

Hence,

$$\frac{dx_i}{dt} \geq -C x_i, \quad \text{or } \frac{d}{dt}(e^{Ct} x_i) \geq 0, \tag{2.16}$$

so that

$$x_i(\tau) > e^{-C\tau} x_i(0). \tag{2.17}$$

This completes the proof by contradiction. □

The system (2.1)–(3.3) satisfies the conditions of Theorem 2.1. Hence, for the appropriate initial conditions, the solutions of the system (2.1)–(3.3) remain nonnegative and bounded.

3. Numerical simulations and results

All computations are performed using the Python ODE solver `odeint()`. In all simulations, we take an initial load of *Plasmodium* parasites, while all other initial values are taken to be close, but not necessarily identical, to their steady state estimated in Section A. The baseline parameters for the simulations are presented in Table 2.

3.1. Simulations without drugs

Figure 2 shows simulations of all the model variables for a virtual malaria patient with no drug treatment. We observe that as the time (t) increases, the concentration of healthy RBCs decreases, while the population of iRBCs initially increases within the first 14 days, and then monotonically decreases. The increase and subsequent decrease of iRBCs correspond to a rise in T cells, which is a response to the infection by *Plasmodium* parasites. The concentration of MIF initially rapidly increases and then gradually thereafter, as it is utilized to regulate the activation of naive RBCs. Notably, PFMIF exhibits dynamics similar to iRBCs and intracellular parasites (P_i).

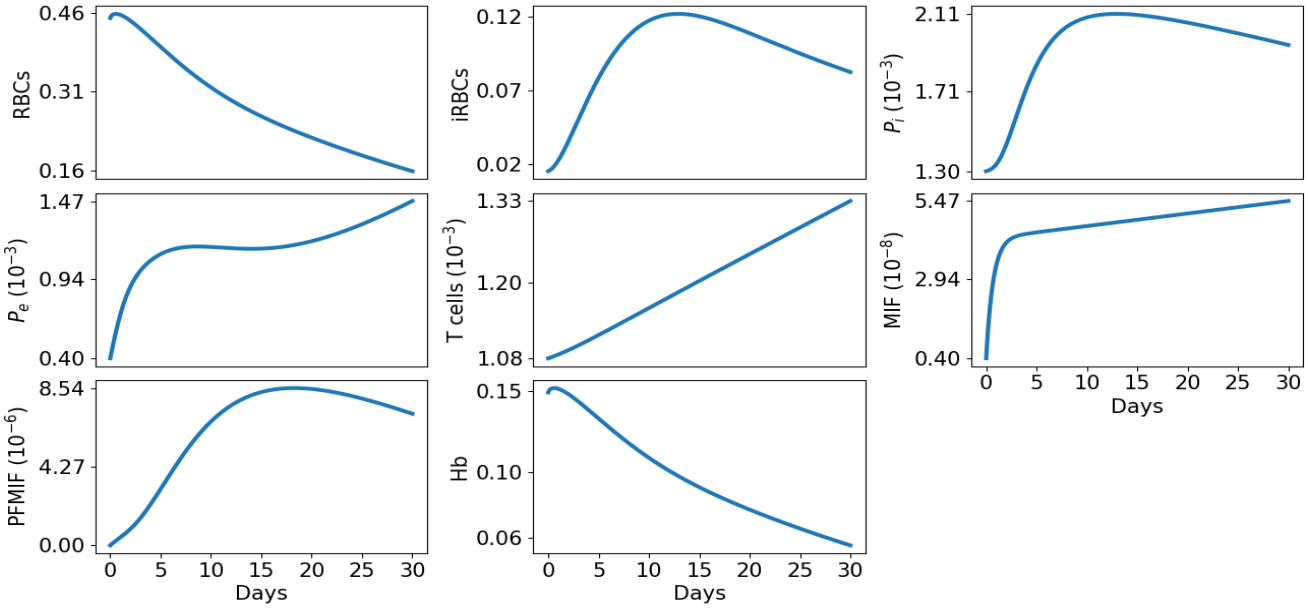

(A) Profiles of all the model variables in the untreated case.

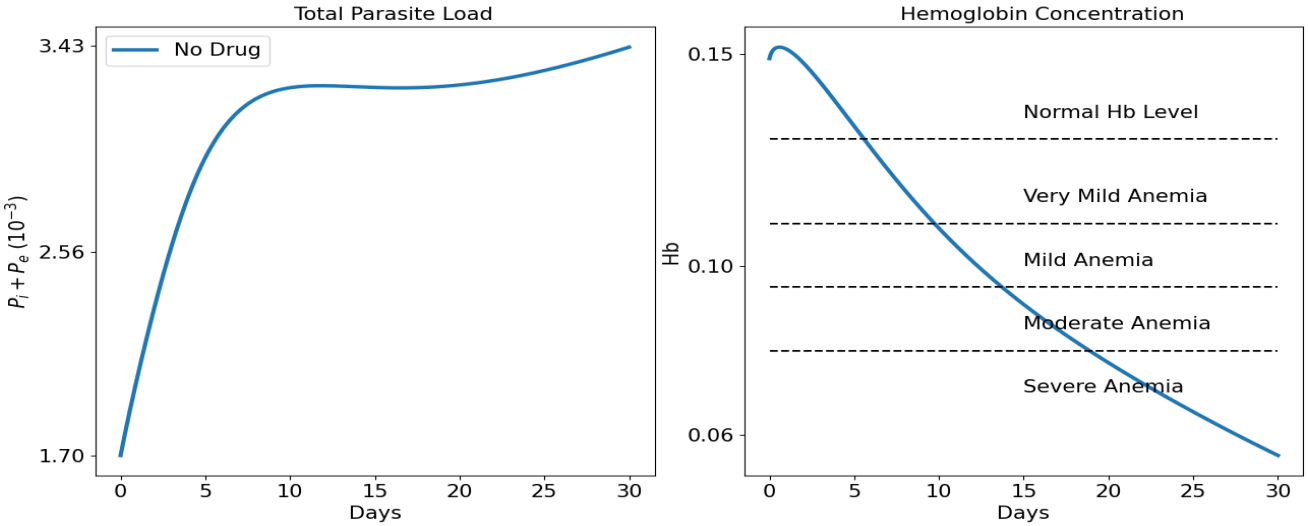

(B) Profiles of total parasite load ($P_i + P_e$) and hemoglobin concentration (H_b).

Figure 2. Simulations for untreated malarial anemia: The patient goes from healthy state (Normal Hb level) to a severe anemia state. All variables are in units of g/ml.

Anemia is a condition characterized by a decrease in hemoglobin levels below the normal range of 0.12–0.18 g/ml due to a reduction in RBCs. Anemia occurs in various levels of severity, including mild anemia (H_b between 0.1–0.12 g/ml), moderate anemia (H_b between 0.08–0.10 g/ml), and severe anemia (H_b <0.08 g/ml) [41–43].

In Figure 2, H_b exhibits a continuous, monotonous decrease, thereby declining from a healthy concentration of approximately 0.15 g/ml to a severe anemia level of around 0.06 g/ml. This decline indicates that without treatment, the virtual patient depicted in Figure 2 will ultimately experience severe anemia due to the *Plasmodium* infection.

3.2. Simulations with anti-malarial drugs

Following the work in [21], we treated the virtual patient in Figure 2 with all combinations of the drugs Artesunate and epoxyazadiradione (Epoxy).

3.2.1. Equation for Artesunate (A) and epoxyazadiradione (E)

We start treatment with both drugs at Day 21 of malaria and give each drug at constant doses per day. We use the PK/PD (pharmacokinetic/pharmacodynamic) model for the drugs.

We denote γ_A as the amount of Artesunate administered at times $t_0 = 21,\ t_1 = 22,\ t_2 = 23$. Hence,

$$C_A(t) = \sum_{j=0}^{k} \gamma_A e^{-\beta_A(t-t_j)} \text{ for } t_{k-1} < t < t_k,\ k = 1, 2, 3, \tag{3.1}$$

where β_A and β_E are some positive parameters. The PD term accounts for depletion of the drug through its effect on iRBCs, namely by enhancing the death of iRBCs. We assume that this term has the form $\lambda_{AB_i} B_i A/(K_A + A)$, where $\lambda_{B_i A}$ is a positive parameter. Then, the dynamic of A takes the following form:

$$\frac{dA}{dt} = \underbrace{C_A(t)}_{\text{source}} - \underbrace{\lambda_{AB_i} B_i \frac{A}{K_A + A}}_{\text{absorption}} - \underbrace{\mu_A A}_{\text{degradation}} \tag{3.2}$$

where $\mu_A A$ is the intrinsic degradation of the drug [44].

The equation for Epoxy has a similar form:

$$\frac{dE}{dt} = \underbrace{C_E(t)}_{\text{source}} - \underbrace{(\lambda_{EB} B + \lambda_{ET_C} T_c) \frac{E}{K_E + E}}_{\text{absorption}} - \underbrace{\mu_E E,}_{\text{degradation}} \tag{3.3}$$

where $C_E(t)$ = has the same form as $C_A(t)$ with some parameters γ_E and β_E.

Figure 3 shows simulations of the total parasite load ($P_1 + P_e$, Figure 3A) and the hemoglobin concentration (H_b, Figure 3B) in a malaria patient under treatment with various combinations of Artesunate and Epoxy.

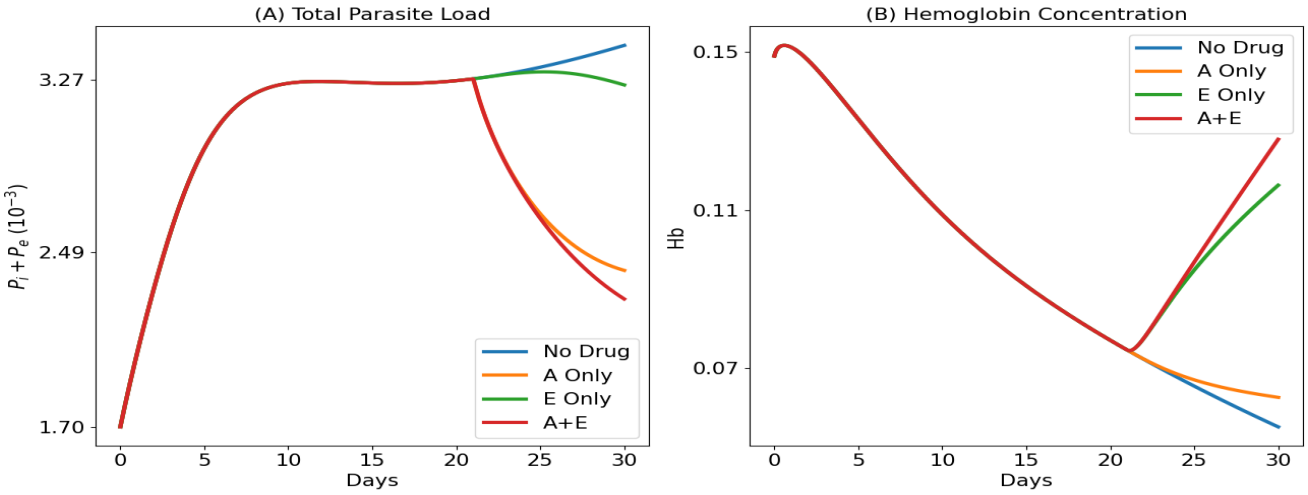

Figure 3. Treatment of severe malarial anemia with combinations of Artesunate and epoxyazadiradione. (A) The total parasite load is significantly decreased when Artesunate is given, and not so much otherwise. (B) The concentration of hemoglobin is significantly increased when epoxyazadiradione is given, and not so much otherwise.

Observations from Figure 3A reveal that $P_i + P_e$ decreases to less than half of its level in the absence of any medication when Artesunate is administered. Furthermore, this reduction in the overall parasite load is further enhanced when Artesunate is used in combination with Epoxy. In contrast, treatment with Epoxy alone yields only a modest decrease in the total parasite load when compared to the no-drug scenario.

On the other hand, as observed in Figure 3B, hemoglobin (H_b) levels rise from their low value (approximately 0.06 g/ml) in the no-drug scenario, which is equivalent to severe anemia, to a level indicative of mild anemia (around 0.12 g/ml) under treatment with Epoxy alone. Furthermore, when treated with a combination of Artesunate and Epoxy, hemoglobin level returns to its normal range (greater than 0.12 g/ml). In contrast, treatment with Artesunate alone results in only a modest increase in hemoglobin levels as compared to the no-drug condition.

These findings align with empirical data documented in references such as [16, 45, 46], thereby corroborating the observations reported in [21].

3.2.2. Simulations with drugs and immune boosters

The effect of immune boosters on malaria therapy refers to the impact of either substances or interventions that enhance the body's immune response in the context of treating malaria. These immune boosters can include vaccines [47], immunomodulatory drugs [48], or strategies aimed at strengthening the host's immune system to better combat the malaria parasite [49]. The goal is to improve the effectiveness of malaria treatments and reduce the severity of the disease.

We represent the immune booster by pulsing the dynamics of T_c, that is, we modify Eq (2.5) as follows:

$$\frac{dT_c}{dt} = \underbrace{C_{T_c}(t)}_{\text{booster}} + \underbrace{\left(\lambda_{T_cB_i}\frac{B_i}{K_{B_i}+B_i} + \lambda_{T_cP_i}\frac{P_i}{K_{P_i}+P_i} + \lambda_{T_cP_e}\frac{P_e}{K_{P_e}+P_e}\right)T_c^0}_{\text{proliferation}}$$

$$\underbrace{-\left(\mu_{T_c} + \mu_{T_c P_f} \frac{P_f}{K_{P_f} + P_f} \frac{1}{1 + E/K_E}\right) T_c}_{\text{death}} \tag{3.4}$$

where $C_{T_c}(t) = \gamma_{T_c}$, which is a constant when the booster is given, and 0 otherwise.

In Figure 4, we model the impact of an immune booster in conjunction with the anti-malarial drugs Artesunate and Epoxy for the virtual patient depicted in Figure 2.

As demonstrated in Figure 4A, the immune booster substantially enhances the effectiveness of Artesunate treatment by reducing the overall parasite load to approximately half of the parasite count at Day 30, in contrast to the case of Artesunate treatment alone. However, this significant improvement in parasite reduction does not correspond to a similar enhancement in hemoglobin dynamics.

In Figure 4B, where the immune booster is employed in conjunction with Epoxy, and in Figure 4C, where the immune booster is combined with both Artesunate and Epoxy, we observe a similar trend to Figure 4A as far as parasitemia is concerned. The immune booster consistently and significantly enhances the reduction of parasitemia. However, while the concentration of hemoglobin remains lower than that under treatment with either Epoxy alone or Epoxy combined with Artesunate, there is a notable improvement in H_b compared to the scenario with no treatment.

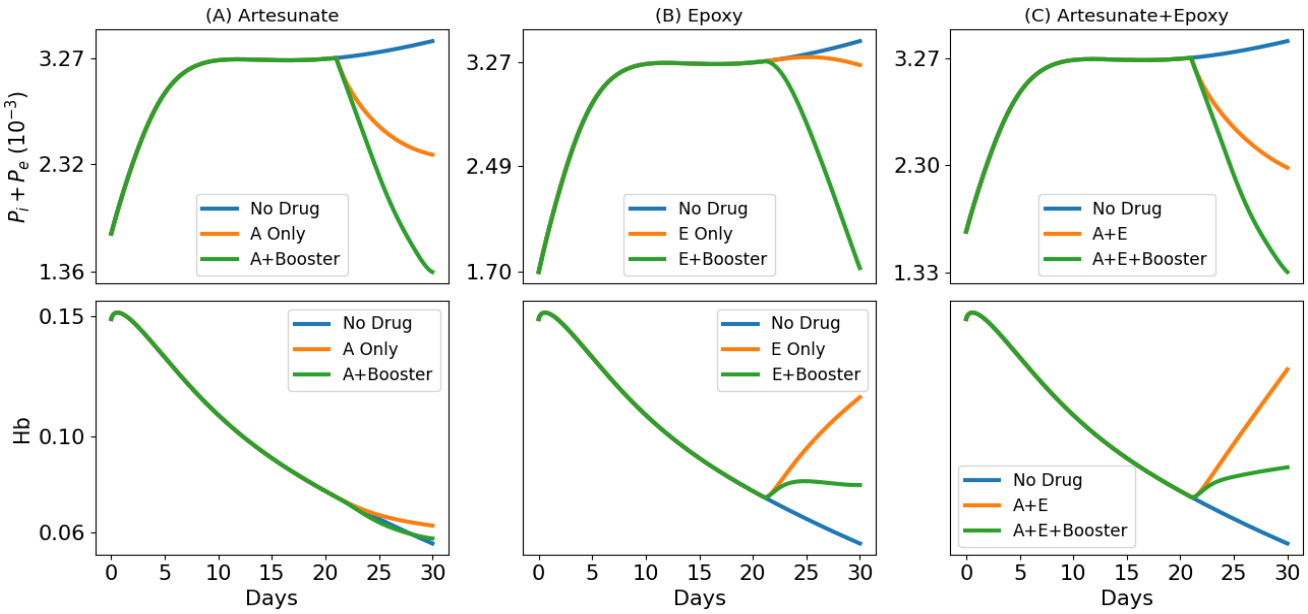

Figure 4. Immune booster and anti-malarial drugs. Association of immune booster with (A) Artesunate alone, (B) epoxyazadiradione alone, and (C) combination of Artesunate and epoxyazadiradione.

3.3. Optimizing the anti-malarial drug and immune booster doses

We use a combination of Artesunate and Epoxy and assess the optimal doses of these drugs in conjunction with immune booster doses that yield a maximum decrease in parasitemia, while maintaining the hemoglobin concentration at a normal level.

In Figure 5, we present a heatmap illustrating the reduction in parasitemia under treatment with Artesunate+Epoxy+booster versus the no-drug case at Day 30. We vary the doses of the drugs (γ_A and γ_E) simultaneously by a factor and the booster (γ_{T_c}) (Figure 5A). The corresponding plot of hemoglobin concentration is provided in Figure 5B.

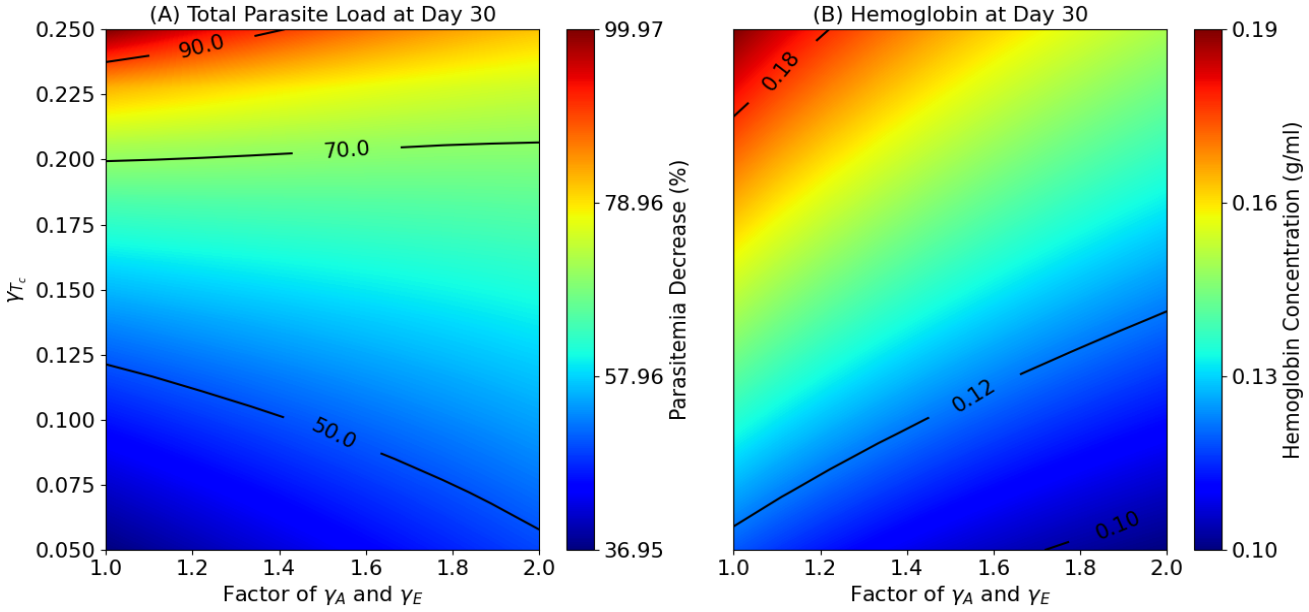

Figure 5. Optimizing the doses for anti-malarial drugs and immune booster. (A) Percentage decrease in total parasite load at Day 30 and (B) hemoglobin concentration at Day 30.

We notice that when γ_A, γ_E, and γ_{T_c} have small values, the reduction in parasitemia remains minimal, thereby leading to a persistently high total parasite load. As a consequence, the hemoglobin concentration decreases. Interestingly, increasing the values of γ_A and γ_E while keeping γ_{T_c} small actually exacerbates the anemia condition.

Large enough values of γ_{T_c} result in optimal parasitemia reduction when γ_A and γ_E are small enough. However, this combination may lead to abnormally high hemoglobin levels (> 1.8 g/ml), unless γ_A and γ_E are appropriately chosen.

4. Discussion and conclusions

Malaria is a disease that has remained a threat to human and animal populations; millions of lives are lost every year due to this disease. The disease may result in severe anemia when the parasite causes a marked reduction in RBC count, thereby leading to a decrease in the hemoglobin level. Artesunate is the first line treatment for severe malaria anemia because it is effective in killing the malaria parasites (*Plasmodium*), thus reducing the parasite load in the blood. However, in the process of killing the parasites in the blood, Artesunate also contributes to the destruction of RBCs, thereby causing a decrease in hemoglobin level, hence causing anemia.

In this work, we developed a mathematical model of within-host interactions between the *Plasmodium*, the RBCs (i.e., healthy RBCs and iRBCs), the macrophages and the T cells that are involved in the

immune response to malaria. To avoid a blood transfusion, which is often applied in severe malarial anemia cases, we proposed to combine Artesunate with an experimental drug, Epoxy, which increases the level of hemoglobin in the blood. Our model simulations in Figure 3 confirm that, when used in a single regimen, the drugs Artesunate and Epoxy can only either reduce parasitemia for Artesunate, which has a mild effect on hemoglobin level, or increase in the hemoglobin level for Epoxy, which has a rather small effect on parasitemia. However, our model simulations suggest that combining Artesunate with Epoxy could effectively reduce the parasite load while maintaining a high enough hemoglobin level, thus treating the patient and avoiding anemia.

The primary results of this paper were previously obtained in a recent article [21], where the authors used a more complex model that included all the variables of our model in addition to various cytokines such as IL-12, IFN-γ and TNF-α, which regulate the activities of the cells. Thus, our model is a simplified version of the model in [21] with comparable results. The purpose of the modification was to reduce the complexity in terms of reducing the number of equations, variables and parameters, thereby resulting in an easier simulation, analysis, interpretation and computational efficiency, while maintaining the essential features.

In malaria infection, as in most pathogenic diseases, the patient's immune system plays a crucial role in combating the pathogens. Immune boosters can help strengthen the immune response, making it more effective in targeting and eliminating the malaria parasites [47–49]. In our model, we represented an immune booster as an impulse in the T cells dynamics, at a constant amount γ_{T_c}. Then, we simulated cases of severe malaria treatment with combinations of the drugs Artesunate (at dose γ_A) and Epoxy (at dose γ_E), where the immune booster is given in conjunction with the two drugs. We obtained the following results:

(i) Small enough amounts of γ_A, γ_E, and γ_{T_c} result in very large parasitemia and a significantly reduced hemoglobin level.

(ii) For a γ_{T_c} large enough, parasitemia is generally significantly decreased, and this decrease is optimal when γ_A and γ_E are small enough. However, in this case, the hemoglobin level may increase to an abnormally large level.

(iii) The most effective combination of Artesunate, Epoxy, and an immune booster for achieving the maximum reduction in parasitemia while simultaneously maintaining hemoglobin concentration at normal levels is obtained when γ_{T_c} reaches a significant magnitude, and both γ_A and γ_E are well-balanced, without being excessively large or too small.

In this paper we demonstrated that by combining immune boosters with a combination of standard anti-malarial drugs, such as Artesunate and epoxyazadiradione, we can significantly improve the efficacy of treatment. However, these conclusions will need to be confirmed in actual clinical trials, with additional attention to potential side effects.

Appendix A

A. Parameters estimations

Most of the parameters of the variables shown in Table 2 are estimated based on the main article and previous studies [40, 50–57]. For simplicity, we assume that

$$Y\frac{S}{K_S + S} = Y\frac{1}{2}$$

for any expression where Y is stimulated by S, and the parameter K_S is the half-saturation of S [21]. Half-saturation, which signifies the point where half of the maximum intake is obtained, is an essential factor in determining the results of models [58]. We will solve for the missing parameters using the time-average steady state equations, with $S^o = K_S$ and $S^o = S$. The values of S^0 are estimated from both experimental and clinical information. We will use the parameters from Table 2 to solve for the following parameters:

Estimate for N_B and n_B

The number of merozoites produced after the rupturing of an infected RBC is approximately 16 to 32 merozoites. We take N_B to be 24. In addition, n_B is the average number of intracellular merozoites inside one infected RBC, which can be as low as 4 or as high as 32 depending on the type of malaria parasite hence, we take $n_B = 6$ [59].

Estimate for m_{M_f}

The mass of one MIF is approximately $m_{M_f} = 2.1\times10^{-20}$ and mass of one red blood cell is 27×10^{-12}. Hence,

$$m_{M_f} = \frac{\text{mass of 1 MIF}}{\text{mass of 1 RBC}} = 7.7 \times 10^{-10}.$$

Estimate for μ_B

The half-life of RBCs in a human being is approximately 120 days [60]. The half-life means that half of the population of RBCs, namely the older RBCs, will no longer be in circulation and will be replaced by new RBCs. We calculate the natural death of red blood cells as follows:

$$\mu_B = \frac{\ln\ 2}{t_H},$$

where $t_H = 120$ days; therefore,

$$\mu_B = \frac{0.693}{120} = 5.78 \times 10^{-3}\ \text{d}^{-1}.$$

Estimate for μ_{P_e}

The half-life of the extracellular merozoites after being released by the infected RBCs is approximately five min [61]. We take $t_H = 1.38 \times 10^{-3}$ day (2 min),

$$\mu_{P_e} = \frac{0.693}{1.38 \times 10^{-3}} = 4.9 \times 10^2\ \text{d}^{-1}.$$

Estimation for production/activation in steady state

Estimate for λ_B

In the human steady state of health, Eq (2.1) implies that the production and death of RBCs are equal, which is $\lambda_B = \mu_B$. In this case, we assume that the rate of production is higher than the rate of death and take $\lambda_B = 2\mu_B$. Therefore,

$$\lambda_B = 1.15 \times 10^{-2}\ \mathrm{d}^{-1}.$$

Estimate for $\lambda_{B_iT_c}$

Solving Eq (2.2) of iRBCs in average time steady state, becomes the following:

$$\lambda_{BB_i} BP_e - \frac{\lambda_{P_iP_e} B_i}{2} - \lambda_{B_iT_c} T_c B_i - \frac{\mu_{B_iA}}{2} B_i - \mu_{B_i} B_i = 0. \tag{A.1}$$

We assume that the presence of Artesunate increases the natural death of iRBCs by 20 [62], hence we take

$$\frac{\mu_{B_iA}}{2} = 20\mu_{B_i}.$$

Equation (A.1) becomes the following:

$$\lambda_{BB_i} BP_e - \frac{\lambda_{P_iP_e} B_i}{2} - \lambda_{B_iT_c} T_c B_i - 40\mu_{B_i} B_i - \mu_{B_i} B_i = 0. \tag{A.2}$$

We have that $\mu_{B_i} = 2.43 \times 10^{-3}\ \mathrm{d}^{-1}$, $\lambda_{BB_i} = 1.44 \times 10^3\ \mathrm{ml/g\ d}^{-1}$, $B_i = K_{B_i} = 0.015$ g/ml, $P_e = K_{P_e} = 4 \times 10^{-4}$g/ml, $T_c = K_{T_c} = 1.08 \times 10^{-3}$g/ml and $\lambda_{P_iP_e} = 0.66\ \mathrm{d}^{-1}$ from Table 2.

$$\lambda_{B_iT_c} = \frac{0.2592 - 6.445 \times 10^{-3}}{1.62 \times 10^{-5}} = 1.5602 \times 10^{-6}\ \mathrm{ml/g\ d}^{-1}.$$

Estimate for $\lambda_{P_iT_c}$

The average time steady state of Eq (2.3) is as follows:

$$\lambda_{p_i} P_i\left(1 - \frac{P_i}{C_a}\right) + \lambda_{BB_i} m_B^* BP_e - \lambda_{P_iP_e} m_B^* N_B B_i \frac{P_i^2}{(m_B^* N_B B_i)^2 + P_i^2} - \lambda_{P_iT_c} \frac{P_i}{K_{P_i} + P_i} T_c$$
$$- \mu_{B_i} n_B P_i = 0,$$

Let $\frac{P_i}{C_a} = \frac{K_{P_i}}{C_{P_i}}$ and $K_{P_i} \simeq m_B^* N_B B_i$, hence, $\frac{P_i^2}{(m_B^* N_B B_i)^2 + P_i^2} = \frac{1}{2}$. We have that $\mu_{B_i} = 2.43 \times 10^{-3}\ \mathrm{d}^{-1}$, $\lambda_{BB_i} = 1.44 \times 10^3\ \mathrm{ml/g\ d}^{-1}$, $B_i = K_{B_i} = 0.015$ g/ml, $P_e = K_{P_e} = 4 \times 10^{-4}$ g/ml, $P_i = K_{P_i} = 1.3 \times 10^{-3}$ g/ml, $n_B = 6$, $T_c = K_{T_c} = 1.08 \times 10^{-3}$ g/ml, $\mu_{B_iA} n_B B_i \frac{A}{A + K_A} = 0$ because there is no treatment yet and $\lambda_{P_iP_e} = 0.66\ \mathrm{d}^{-1}$ from Table 2.

$$3.18 \times 1.3 \times 10^{-3} + 1.44 \times 10^3 \times 3.7 \times 10^{-3} \times 0.45 \times 4 \times 10^{-4} - \frac{0.66 \times 1.3 \times 10^{-3}}{2}$$
$$- \frac{\lambda_{P_iT_c} 1.08 \times 10^{-3}}{2} - 2.43 \times 10^{-3} \times 6 \times 1.3 \times 10^{-3} = 0.$$

Hence,

$$\lambda_{P_iT_c} = 4.845 \times 10^{-8}\ \mathrm{d}^{-1}.$$

Estimate for $\lambda_{P_eT_c}$

We assume that T cells are capable of killing extracellular parasites at a rate that is five times faster than their ability to kill intracellular parasites because extracellular parasites are more readily accessible. Therefore we have the following:

$$\lambda_{P_eT_c} = 2.425 \times 10^{-7}\ \mathrm{d}^{-1}.$$

Estimates for $\lambda_{T_cB_i}$, $\lambda_{T_cP_e}$ and $\lambda_{T_cP_i}$

We write Eq (2.5) in its time average steady state without treatment in the following form:

$$\left(\frac{\lambda_{T_cB_i}}{2} + \frac{\lambda_{T_cP_i}}{2} + \frac{\lambda_{T_cP_e}}{2}\right)T_c^0 - \left(\mu_{T_c} + \frac{\mu_{T_cP_f}}{2}\right)T_c = 0. \tag{A.3}$$

We assume that extracellular parasites are more effective in activating the T cells than intracellular parasites during the infection of malaria; therefore, we take $\lambda_{T_cP_e} = 2\lambda_{T_cB_i}$. Since intracellular parasites are hidden inside the iRBCs, we can assume that $\lambda_{T_cP_i} = \lambda_{T_cB_i}$. Hence, Eq (A.3) becomes the following:

$$(4\lambda_{T_cB_i})T_c^0 - \left(2\mu_{T_c} + \mu_{T_cP_f}\right)T_c = 0, \tag{A.4}$$

with $T_c^0 = 1.08 \times 10^{-3}$ g/ml, $\mu_{T_c} = 0.197\ \mathrm{d}^{-1}$, $\mu_{T_cP_f} = 2 \times 10^9\ \mathrm{d}^{-1}$ and $T_c = K_{T_c} = 1.08 \times 10^{-3}$ g/ml from Table 2. Replacing the values in Eq (A.4), we obtain the following:

$$4.32 \times 10^{-3}\lambda_{T_cB_i} = (0.394 + 2 \times 10^9)1.08 \times 10^{-3}.$$

Hence,

$$\lambda_{T_cB_i} = 5 \times 10^2\ \mathrm{d}^{-1}.$$

We took $\lambda_{T_cP_e} = 2\lambda_{T_cB_i}$; therefore, $\lambda_{T_cP_e} = 1 \times 10^3\ \mathrm{d}^{-1}$ and $\lambda_{T_cB_i} = \lambda_{T_cP_i} = 5 \times 10^2\ \mathrm{d}^{-1}$.

Estimate for C_A

From Eq (3.2), C_A represents the dosage of the drug Artesunate administered per day. Before administering the drug, some factors need to be considered: the patient's weight, the duration of treatment, the number of days the medication will be given and the number of doses. An average adult weighs between 60 and 80 kg and has a blood volume of approximately 5 liters. In this situation, Artesunate will be administered intravenously to ensure that the medication is quickly delivered to the targeted area of the body [63]. The recommended dosage for this medication is 2.4 mg/kg intravenously at 0, 12, and 24 hours [64]. For simplicity, instead of considering the drug dose at each time t_i we take the average of 1 day. Taking the units for the drug dosage into grams, we obtain 0.0024 g/kg. Since this dosage is given per kg of weight, we take 70kg as the weight of an average adult which gives us 0.168 g. Calculating the average volume of blood of a healthy person in milliliters gives the following:

$$5L = 5 \times 10^3\ \mathrm{ml}.$$

Hence, the level of drug administered per day for 4 days is calculated as follows:

$$C_A = \frac{4\ \text{doses}}{4\ \text{days}} \frac{0.168\ g}{5 \times 10^3\ \mathrm{ml}} = 4.4 \times 10^{-5}\ \text{g/ml per day}.$$

We take the dose of Epoxy C_E to be the same since there is no standard dose for its administration. Hence,

$$C_E = 4.4 \times 10^{-5} \text{ g/ml per day.}$$

Use of AI tools declaration

The authors declare they have not used Artificial Intelligence (AI) tools in the creation of this article.

Acknowledgments

This research was supported by the African Institute for Mathematical Sciences (AIMS)-Cameroon, and the School of Mathematics and Statistics at Rochester Institute of Technology.

Conflict of interest

The authors declare that they have no known competing interests that could have appeared to influence the work reported in this paper.

References

1. Snow RW, Korenromp EL, Gouws E (2004) Pediatric mortality in Africa: plasmodium falciparum malaria as a cause or risk? *Am J Trop Med Hyg* 71: 16–24. https://doi.org/10.4269/ajtmh.2004.71.16
2. Ross A, Maire N, Molineaux L, et al. (2006) An epidemiologic model of severe morbidity and mortality caused by Plasmodium falciparum. *Am J Trop Med Hyg* 75: 63–73. https://doi.org/10.4269/ajtmh.2006.75.63
3. Graumans W, Jacobs E, Bousema T, et al. (2020) When is a Plasmodium-infected mosquito an infectious mosquito? *Trends Parasitol* 36: 705–716. https://doi.org/10.1016/j.pt.2020.05.011
4. Beier JC (1998) Malaria parasite development in mosquitoes. *Annu Rev Entomol* 43: 519–543. https://doi.org/10.1146/annurev.ento.43.1.519
5. Kafsack BF, Rovira-Graells N, Clark TG, et al. (2014) A transcriptional switch underlies commitment to sexual development in malaria parasites. *Nature* 507: 248–252. https://doi.org/10.1038/nature12920
6. Fernández-Grandon GM, Gezan SA, Armour JA, et al. (2015) Heritability of attractiveness to mosquitoes. *PloS One* 10: e0122716. https://doi.org/10.1371/journal.pone.0122716
7. Delves M, Plouffe D, Scheurer C, et al. (2012) The activities of current antimalarial drugs on the life cycle stages of Plasmodium: a comparative study with human and rodent parasites. *PLoS Med* 9: e1001169. https://doi.org/10.1371/journal.pmed.1001169
8. Kappe SH, Kaiser K, Matuschewski K (2003) The Plasmodium sporozoite journey: a rite of passage. *Trends Parasitol* 19: 135–143. https://doi.org/10.1016/S1471-4922(03)00007-2

9. Nureye D, Assefa S (2020) Old and recent advances in life cycle, pathogenesis, diagnosis, prevention, and treatment of malaria including perspectives in Ethiopia. *Sci World J* 2020:1–17. https://doi.org/10.1155/2020/1295381
10. Centers for Disease Control and Prevention, The history of malaria, an ancient disease. CDC, 2010. Available from: https://stacks.cdc.gov/view/cdc/135582.
11. McDevitt MA, Xie J, Ganapathy-Kanniappan S, et al. (2006) A critical role for the host mediator macrophage migration inhibitory factor in the pathogenesis of malarial anemia. *J Exp Med* 203: 1185–1196. https://doi.org/10.1084/jem.20052398
12. Sun T, Holowka T, Song Y, et al. (2012) A Plasmodium-encoded cytokine suppresses T-cell immunity during malaria. *P Natl Acad Sci USA* 109: E2117–E2126. https://doi.org/10.1073/pnas.1206573109
13. Wynn AA, Myint O, Zin T (2016) Host and parasite immunopathogenesis of malaria. *Survival* 34: 35.
14. Cordery DV (2007) Characterisation of macrophage migration inhibitory factor homologues in plasmodium species [PhD's thesis]. Open University, United Kingdom.
15. Rosenthal PJ (2008) Artesunate for the treatment of severe falciparum malaria. *N Engl J Med* 358: 1829–1836. https://doi.org/10.1056/NEJMct0709050
16. Burri C, Ferrari G, Ntuku HM, et al. (2014) Delayed anemia after treatment with injectable artesunate in the Democratic Republic of the Congo: a manageable issue. *Am J Trop Med Hyg* 91: 821. https://doi.org/10.4269/ajtmh.14-0149
17. Alam A, Haldar S, Thulasiram HV, et al. (2012) Novel anti-inflammatory activity of epoxyazadiradione against macrophage migration inhibitory factor: inhibition of tautomerase and proinflammatory activities of macrophage migration inhibitory factor. *J Biol Chem* 287: 24844–24861. https://doi.org/10.1074/jbc.M112.341321
18. Olotu A, Urbano V, Hamad A, et al. (2018) Advancing global health through development and clinical trials partnerships: A randomized, placebo-controlled, double-blind assessment of safety, tolerability, and immunogenicity of PfSPZ vaccine for malaria in healthy equatoguinean men. *Am J Trop Med Hyg* 98: 308. https://doi.org/10.4269/ajtmh.17-0449
19. Gupta S, Snow RW, Donnelly CA, et al. (1999) Immunity to non-cerebral severe malaria is acquired after one or two infections. *Nat Med* 5: 340–343. https://doi.org/10.1038/6560
20. Frosch AE, John CC (2012) Immunomodulation in Plasmodium falciparum malaria: experiments in nature and their conflicting implications for potential therapeutic agents. *Expert Rev Anti Infect Ther* 10: 1343–1356. https://doi.org/10.1586/eri.12.118
21. Siewe N, Friedman A (2020) Increase hemoglobin level in severe malarial anemia while controlling parasitemia: A mathematical model. *Math Biosci* 326: 108374. https://doi.org/10.1016/j.mbs.2020.108374
22. Cooper B (2011) The origins of bone marrow as the seedbed of our blood: from antiquity to the time of Osler. *Bayl Univ Med Cent* 24: 115–118. https://doi.org/10.1080/08998280.2011.11928697
23. Cowman AF, Tonkin CJ, Tham WH, et al. (2017) The molecular basis of erythrocyte invasion by malaria parasites. *Cell Host Microbe* 22: 232–245. https://doi.org/10.1016/j.chom.2017.07.003

24. Cowman AF, Crabb BS (2006) Invasion of red blood cells by malaria parasites. *Cell* 124: 755–766. https://doi.org/10.1016/j.cell.2006.02.006

25. Birkle T, Brown G (2021) I'm infected, eat me! Innate immunity mediated by live, infected cells signaling to be phagocytosed. *Infect Immun* 89: e00476-20. https://doi.org/10.1128/IAI.00476-20

26. Alzoubi K, Calabrò S, Bissinger R, et al. (2014) Stimulation of suicidal erythrocyte death by artesunate. *Cell Physiol Biochem* 34: 2232–2244. https://doi.org/10.1159/000369666

27. Fernandes P, Loubens M, Le Borgne R, et al. (2022) The AMA1-RON complex drives Plasmodium sporozoite invasion in the mosquito and mammalian hosts. *PLoS Pathog* 18: e1010643. https://doi.org/10.1371/journal.ppat.1010643

28. Aggarwal R, Chamoli A, Rawat M, et al. (2023) A review on malaria, its control and management. *AJPSci*. https://doi.org/10.52711/2231-5659.2023.00027

29. Antonelli LR, Junqueira C, Vinetz JM, et al. (2020) The immunology of Plasmodium vivax malaria. *Immunol Rev* 293: 163–189. https://doi.org/10.1111/imr.12816

30. Elmore S (2007) Apoptosis: a review of programmed cell death. *Toxicol Pathol* 35: 495–516. https://doi.org/10.1080/01926230701320337

31. Junqueira C, Polidoro RB, Castro G, et al. (2021) $\gamma\delta$ T cells suppress Plasmodium falciparum blood-stage infection by direct killing and phagocytosis. *Nat Immunol* 22: 347–357. https://doi.org/10.1038/s41590-020-00847-4

32. Kumar R, Loughland JR, Ng SS, et al. (2020) The regulation of CD4+ T cells during malaria. *Immunol Rev* 293: 70–87. https://doi.org/10.1111/imr.12804

33. Alimonti JB, Ball TB, Fowke KR (2003) Mechanisms of CD4+ T lymphocyte cell death in human immunodeficiency virus infection and AIDS. *J Gen Virol* 84: 1649–1661. https://doi.org/10.1099/vir.0.19110-0

34. Calandra T, Spiegel LA, Metz CN, et al. (1998) Macrophage migration inhibitory factor is a critical mediator of the activation of immune cells by exotoxins of Gram-positive bacteria. *P Natl Acad Sci USA* 95: 11383–11388. https://doi.org/10.1073/pnas.95.19.11383

35. Tarasuk M, Poungpair O, Ungsupravate D, et al. (2014) Human single-chain variable fragment antibody inhibits macrophage migration inhibitory factor tautomerase activity. *Int J Mol Med* 33: 515–522. https://doi.org/10.3892/ijmm.2014.1622

36. Augustijn KD, Kleemann R, Thompson J, et al. (2007) Functional characterization of the Plasmodium falciparum and P. berghei homologues of macrophage migration inhibitory factor. *Infect Immun* 75: 1116–1128. https://doi.org/10.1128/IAI.00902-06

37. Schipper S, Springer E, Hahn J, et al. (2022) Characterization of Plasmodium falciparum macrophage migration inhibitory factor homologue and its cysteine deficient mutants. *Parasitol Int* 87: 102513. https://doi.org/10.1016/j.parint.2021.102513

38. Brundha M, Pathmashri V, Sundari S (2019) Quantitative changes of red blood cells in cancer patients under palliative radiotherapy-a retrospective study. *Res J Pharm Technol* 12: 687–692. https://doi.org/10.5958/0974-360X.2019.00122.7

39. Stadler AM, Digel I, Artmann GM, et al. (2008) Hemoglobin dynamics in red blood cells: correlation to body temperature. *Biophys J* 95: 5449–5461. https://doi.org/10.1529/biophysj.108.138040

40. Siewe N, Yakubu AA, Satoskar AR, et al. (2016) Immune response to infection by leishmania: A mathematical model. *Math Biosci* 276: 28–43. https://doi.org/10.1016/j.mbs.2016.02.015

41. Ludwig H, Strasser K (2001) Symptomatology of anemia. *Semin Oncol* 28: 7–14. https://doi.org/10.1016/S0093-7754(01)90206-4

42. Otto JM, Montgomery HE, Richards T (2013) Haemoglobin concentration and mass as determinants of exercise performance and of surgical outcome. *Extrem Physiol Med* 2: 1–8. https://doi.org/10.1186/2046-7648-2-33

43. Kariyeva GK, Magtymova A, Sharman A (2000) Turkmenistan demographic and health survey: Anemia. *DHS* 12: 141–147.

44. Ruwizhi N, Maseko RB, Aderibigbe BA (2022) Recent advances in the therapeutic efficacy of artesunate. *Pharmaceutics* 14: 504. https://doi.org/10.3390/pharmaceutics14030504

45. Eltahir HG, Bilal JA, Ali EA, et al. (2017) No reduction in hemoglobin level in severe plasmodium falciparum malaria treated with artesunate in central Sudan. *J Trop Pediatr* 63: 18–22. https://doi.org/10.1093/tropej/fmw041

46. Rehman K, Lötsch F, Kremsner PG, et al. (2014) Haemolysis associated with the treatment of malaria with artemisinin derivatives: a systematic review of current evidence. *Int J Infect Dis* 29: 268–273. https://doi.org/10.1016/j.ijid.2014.09.007

47. El-Moamly AA, El-Sweify MA (2023) Malaria vaccines: the 60-year journey of hope and final success—lessons learned and future prospects. *Trop Med Health* 51: 29. https://doi.org/10.1186/s41182-023-00516-w

48. O'Flaherty K, Maguire J, Simpson JA, et al. (2017) Immunity as a predictor of anti-malarial treatment failure: a systematic review. *Malar J* 16: 1–11. https://doi.org/10.1186/s12936-017-1815-y

49. Doolan DL, Dobano C, Baird JK (2009) Acquired immunity to malaria. *Clin Microbiol Rev* 22: 13–36. https://doi.org/10.1128/CMR.00025-08

50. Siewe N, Yakubu AA, Satoskar AR, et al. (2017) Granuloma formation in leishmaniasis: A mathematical model. *J Theor Biol* 412: 48–60. https://doi.org/10.1016/j.jtbi.2016.10.004

51. Siewe N, Friedman A (2022) Cancer therapy with immune checkpoint inhibitor and CSF-1 blockade: A mathematical model. *J Theor Biol* 556: 111297. https://doi.org/10.1016/j.jtbi.2022.111297

52. Siewe N, Friedman A (2022) Combination therapy for mCRPC with immune checkpoint inhibitors, ADT and vaccine: A mathematical model. *PLoS One* 17: e0262453. https://doi.org/10.1371/journal.pone.0262453

53. Siewe N, Friedman A (2023) Breast cancer exosomal microRNAs facilitate pre-metastatic niche formation in the bone: A mathematical model. *Bull Math Biol* 85: 12. https://doi.org/10.1007/s11538-022-01117-0

54. Siewe N, Friedman A (2022) Optimal timing of steroid initiation in response to CTLA-4 antibody in metastatic cancer: A mathematical model. *PLoS One* 17: e0277248. https://doi.org/10.1371/journal.pone.0277248

55. Friedman A, Siewe N (2020) Overcoming drug resistance to BRAF inhibitor. *Bull Math Biol* 82: 1–31. https://doi.org/10.1007/s11538-019-00691-0

56. Siewe N, Friedman A (2021) TGF-β inhibition can overcome cancer primary resistance to PD-1 blockade: a mathematical model. *PLoS One* 16: 1–16. https://doi.org/10.1371/journal.pone.0252620

57. Friedman A, Siewe N (2018) Chronic hepatitis B virus and liver fibrosis: A mathematical model. *PLoS One* 13: 1–23. https://doi.org/10.1371/journal.pone.0195037

58. Mulder C, Hendriks AJ (2014) Half-saturation constants in functional responses. *Glob Ecol Conserv* 2: 161–169. https://doi.org/10.1016/j.gecco.2014.09.006

59. Kamangira B, Nyamugure P, Magombedze G (2014) A theoretical mathematical assessment of the effectiveness of coartemether in the treatment of Plasmodium falciparum malaria infection. *Math Biosci* 256: 28–41. https://doi.org/10.1016/j.mbs.2014.07.010

60. Quinlivan EP (2008) Calculation of steady state conditions and elimination kinetics of red blood cell folate in women of childbearing age after daily supplementation with various forms and doses of folate. *Am J Clin Nutr* 87: 1537–1538. https://doi.org/10.1093/ajcn/87.5.1537

61. Boyle MJ, Wilson DW, Richards JS, et al. (2010) Isolation of viable Plasmodium falciparum merozoites to define erythrocyte invasion events and advance vaccine and drug development. *P Natl Acad Sci USA* 107: 14378–14383. https://doi.org/10.1073/pnas.1009198107

62. Li Q, Weina P (2010) Artesunate: the best drug in the treatment of severe and complicated malaria. *Pharmaceuticals* 3: 2322–2332. https://doi.org/10.3390/ph3072322

63. Zoller T, Junghanss T, Kapaun A, et al. (2011) Intravenous artesunate for severe malaria in travelers, Europe. *J Clin Invest* 17: 771–777. https://doi.org/10.3201/eid1705.101229

64. World Health Organization (2000) *Management of Severe Malaria: a Practical Handbook*, World Health Organization.

AIMS Press